EPJ Web of Conferences **364**, 02006 (2026) https://doi.org/10.1051/epjconf/202636402006
Quark Matter 2025

Charmonium production in Pb–Pb collisions at forward rapidity in ALICE

Sara Garetti[1,2,*] on behalf of the ALICE Collaboration

[1]IJCLab
[2]Université Paris-Saclay, France

Abstract. Quarkonium production in high-energy collisions is a valuable tool to study both perturbative and non-perturbative aspects of QCD. Charmonia, such as the J/ψ and ψ(2S), are bound states of charm and anti-charm quarks. The ψ(2S), being less bound than the J/ψ, is more sensitive to the quark-gluon plasma (QGP) formed in heavy-ion collisions. Its suppression relative to the J/ψ can reveal how different states are modified in the QGP. The ψ(2S) to J/ψ yield ratio in Pb–Pb, compared to pp collisions, helps isolate medium effects.
In this article, the current status of the analysis of inclusive J/ψ and ψ(2S) production at forward rapidity ($2.5 < y < 4$) in Pb–Pb collisions at a center-of-mass energy per nucleon pair of $\sqrt{s_{\rm NN}} = 5.36$ TeV is presented. The study is based on 2023 data obtained with the upgraded ALICE apparatus during LHC Run 3, using a larger data sample with respect to the results from Run 2. The ψ(2S)-to-J/ψ ratio is presented as a function of the charmonium transverse momentum ($p_{\rm T}$) and event centrality and is compared to the extrapolated ratio from pp collisions, and to existing theoretical models.

1 Introduction

A Large Ion Collider Experiment (ALICE) at the LHC investigates nuclear matter under extreme energy densities, where the formation of a quark-gluon plasma (QGP) is expected. Charmonia are bound states consisting of a charm and an anti-charm quark. Their production process can be broken down into two stages: the production of the heavy quarks and the formation of the bound state. The first stage occurs during initial hard parton-parton scatterings with large momentum transfer, which can be described using perturbative QCD (e.g., $gg \rightarrow c\bar{c}$). The second stage, involving long-distance interactions and soft momentum scales, is a non-perturbative process.

In Pb–Pb collisions at LHC energies, charmonium production is influenced by several hot nuclear matter effects, such as suppression due to color screening [1], regeneration from abundant $c\bar{c}$ pairs [2, 3], and parton energy loss [4]. Cold nuclear matter effects, including gluon shadowing [5], may also play a role. Since the ψ(2S) is more loosely bound than the J/ψ, its production rate relative to the J/ψ in the medium can provide insights into the effects of the deconfined phase. The double ratio of ψ(2S) to J/ψ in Pb–Pb relative to pp collisions helps quantify the relative modifications of these two states, offering a clearer picture of the properties of the QGP via its impact on different charmonium states.

*e-mail: sara.garetti@cern.ch

In this article the analysis of inclusive J/ψ and ψ(2S) production at forward rapidity (2.5 $< y <$ 4) in Pb–Pb collisions at a center-of-mass energy per nucleon pair of $\sqrt{s_{\rm NN}}$ = 5.36 TeV is presented. The analysis is based on the data collected in 2023 with the upgraded ALICE apparatus during LHC Run 3, providing a factor of about 2 larger data sample with respect to Run 2.

2 Experimental apparatus

The analysis presented here uses three of the ALICE subsystems: the Inner Tracking System (ITS) for tracking and vertexing, the Fast Interaction Trigger (FT0) for centrality determination, and the Muon Spectrometer (MS). The MS consists of a front absorber, a dipole magnet, ten planes of muon chambers (MCH), used to track the muons and reconstruct their momenta, an iron wall, and four planes of Muon IDentifier (MID) chambers. Since Run 3 the ALICE MS includes also the Muon Forward Tracker (MFT), which improves tracking and vertex finding and will be used in future studies to separate the prompt and non-prompt contributions of charmonia in Pb–Pb analyses.

3 Analysis Steps

The goal of the analysis is to measure the inclusive ψ(2S)-to-J/ψ ratio in Pb–Pb collisions, defined as

$$\frac{\mathrm{BR}_{\mathrm{J}/\psi} \cdot \sigma_{\mathrm{J}/\psi}}{\mathrm{BR}_{\psi(2\mathrm{S})} \cdot \sigma_{\psi(2\mathrm{S})}} = \frac{N_{\mathrm{J}/\psi}/(A \times \epsilon)_{\mathrm{J}/\psi}}{N_{\psi(2\mathrm{S})}/(A \times \epsilon)_{\psi(2\mathrm{S})}} \tag{1}$$

where $\mathrm{N}_{\mathrm{J}/\psi}$ and $\mathrm{N}_{\psi(2\mathrm{S})}$ are the yields extracted for the J/ψ and ψ(2S), respectively, $A \times \epsilon$ the acceptance times efficiency of the detectors for the two particles, BR the branching ratios, and $\sigma_{\mathrm{J}/\psi}$ and $\sigma_{\psi(2\mathrm{S})}$ the corresponding inclusive production cross sections.

Both event and track selections are applied to the collected data. The J/ψ and ψ(2S) yields are determined by fitting the opposite-sign dimuon invariant-mass spectrum, after subtracting the combinatorial background estimated with the event-mixing (EM) technique. To obtain the EM invariant-mass distribution, single-muon tracks from different collisions are combined together. Figure 1 shows the dimuon invariant-mass spectrum in case of most central events.

For each centrality and p_{T} interval several fit trials have been performed; the final yields have been estimated as the average of the trial results and the systematics uncertainties on these have been computed as the Root Mean Square of the trial distribution, after rejecting those which didn't meet some pre-defined fit quality requirements (convergence and reduced χ^2). Once the yields are determined, they need to be corrected for the acceptance times efficiency of the detector ($A \times \epsilon$). The $A \times \epsilon$ has been calculated using signals from MC with tuned kinematic distributions from previous measurements [6] and a realistic description of the detector conditions during the Pb–Pb data taking period. The uncertainty associated to the accuracy of the detector description in MC results in a contribution of 2% to the total systematic uncertainties. These are however dominated by signal extraction, and they amount to 8-17 % across centrality intervals and 10-29 % across p_{T} intervals.

To estimate what is expected without medium suppression, the ψ(2S)-to-J/ψ ratio in pp collisions has been extrapolated at the energy of $\sqrt{s}$ = 5.36 TeV from published data [7]. The corresponding rescaled pp ψ(2S) peak is shown in Fig. 1 as dotted blue line. The ψ(2S) yield in Pb–Pb is observed to be about a factor two smaller than in rescaled pp collisions.

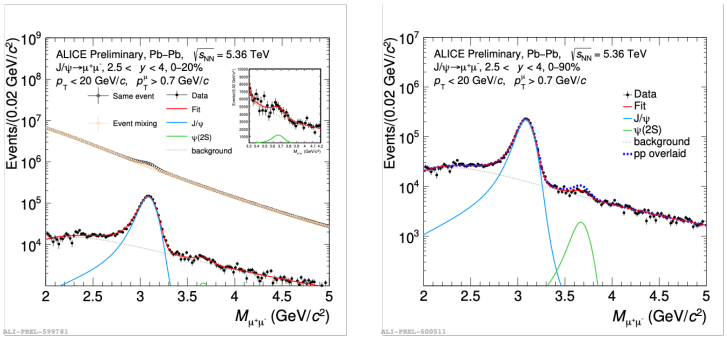

Figure 1. On the left the dimuon invariant-mass spectrum in most central 0–20 % Pb-Pb collisions at $\sqrt{s_{NN}}$ = 5.36 TeV. After the mixed event subtraction from the same event spectrum, the distribution reported in filled black dots is obtained. On the right the same event opposite-sign dimuon invariant-mass spectra, for Pb–Pb collisions, after subtraction of the uncorrelated background is reported as black data points. The pp rescaled ψ(2S) peak is shown as a dotted blue line.

4 Results

The ψ(2S)-to-J/ψ ratios are reported as a function of centrality and p_T in Fig. 2. The ratios measured in Run 3 at $\sqrt{s_{NN}}$ = 5.36 TeV is in good agreement with the ones from Run 2 at $\sqrt{s_{NN}}$ = 5.02 TeV, within the experimental uncertainties. The systematic uncertainties are in general smaller in Run 3 than Run 2 for all considered centrality intervals and for all but on p_T interval. This is attributed to the larger data sample collected in Run 3, which improves the quality of the event-mixing subtraction procedure and of the signal extraction.

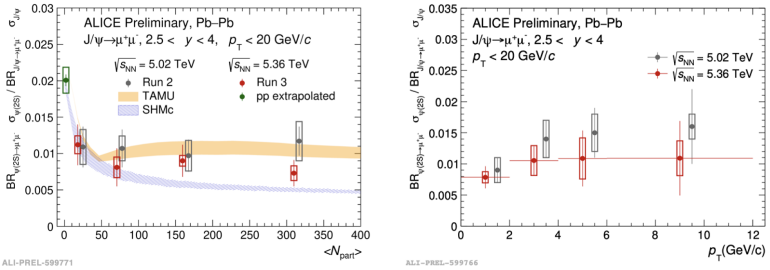

Figure 2. On the left, the ratio of the ψ(2S) to J/ψ cross sections multiplied by the respective BR as a function of $\langle N_{part} \rangle$. On the right, the ratio versus p_T. The vertical error bars are the statistical uncertainties, while the boxes are the systematic ones.

The p_T dependence of the ψ(2S)-to-J/ψ ratio provides insight into the interplay between different production and suppression mechanisms in heavy-ion collisions. At low p_T, recombination may contribute, while color screening is expected across the full p_T range. Within current uncertainties, no significant p_T or centrality dependence is observed.

Figure 2 left shows the centrality dependence compared with the TAMU [8] and SHMc [9] models and with the pp value extrapolated to $\sqrt{s}$ = 5.36 TeV . The ratio is studied versus $\langle N_{part} \rangle$, a proxy for collision centrality, where stronger QGP effects are expected in more central events. Run 2 points are shifted horizontally for clarity.

TAMU includes sequential suppression and possible regeneration, whereas SHMc assumes complete melting of charmonia in the QGP and formation at chemical freeze-out via statistical hadronization. The measured ratio is smaller by about a factor two relative to pp. Both models describe the Run 3 data within uncertainties, while SHMc tends to underestimate the Run 2 results in central events.

5 Conclusions

The ψ(2S)-to-J/ψ yield ratio has been measured in Pb–Pb collisions at $\sqrt{s_{\rm NN}}$ = 5.36 TeV, based on data collected during Run 3 with the ALICE detector. This analysis constitutes the first determination of this observable at this collision energy. The ratio is studied as a function of centrality and transverse momentum, and the results show a good agreement with previous measurements at $\sqrt{s_{\rm NN}}$ = 5.02 TeV from Run 2.

Future developments will include the analysis of the 2024 Pb–Pb dataset and the extraction of the double ratio and the nuclear modification factor ($R_{\rm AA}$) using the pp reference data at $\sqrt{s}$ = 5.36 TeV , also collected in 2024.

The integration of the Muon Forward Tracker into the analysis framework will allow the separation of prompt and non-prompt charmonia and a significant reduction of the combinatorial background, which is essential for a better extraction of the ψ(2S) signal.

References

[1] T. Matsui and H. Satz, J/ψ Suppression by Quark-Gluon Plasma Formation. Phys. Lett. B **178**, 416 (1986). https://doi.org/10.1016/0370-2693(86)91404-8

[2] P. Braun-Munzinger *et al.*, Hadron production in Au - Au collisions at RHIC, Phys. Lett. B **518** (2001), 41-46 https://doi.org/10.1016/S0370-2693(01)01069-3

[3] R. L. Thews, M. Schroedter and J. Rafelski, Enhanced J/ψ production in deconfined quark matter. Phys. Rev. C **63**, 054905 (2001). https://doi.org/10.1103/PhysRevC.63.054905

[4] F. Arleo, Quenching of Hadron Spectra in Heavy Ion Collisions at the LHC, Phys. Rev. Lett. **119** (2017) no.6, 062302. https://doi.org/10.1103/PhysRevLett.119.062302

[5] N. Armesto, Nuclear shadowing. J. Phys. G **32**, R367–R394 (2006). https://doi.org/10.1088/0954-3899/32/11/R01

[6] S. Acharya et al. (ALICE Collaboration), ψ(2S) Suppression in Pb-Pb Collisions at the LHC. Phys. Rev. Lett. **04**, 132 (2024). https://link.aps.org/doi/10.1103/PhysRevLett.132.042301

[7] S. Acharya *et al.* [ALICE], Inclusive quarkonium production in pp collisions at $\sqrt{s}$ = 5.02 TeV, Eur. Phys. J. C **83** (2023) no.1, 61 https://doi.org/10.1140/epjc/s10052-022-10896-8

[8] X. Du and R. Rapp, Sequential regeneration of charmonia in heavy-ion collisions, Nucl. Phys. A **943**, 147 (2015). https://doi.org/10.1016/j.nuclphysa.2015.09.006

[9] A. Andronic *et al.*, Transverse momentum distributions of charmonium states with the statistical hadronization model, Phys. Lett. B **797** (2019), 134836 https://doi.org/10.1016/j.physletb.2019.134836